photonics

MDPI

Article

Modeling and Optimization of NLOS Underwater Optical Channels Using QAM-OFDM Technique

Noor Abdulqader Hamdullah [1,*], Mesut Çevik [1], Hameed Mutlag Farhan [1] and İzzet Paruğ Duru [2]

[1] Department of Electrical and Computer Engineering, Altınbaş University, Istanbul 34217, Türkiye; mesut.cevik@altinbas.edu.tr (M.Ç.); hameed.farhan@altinbas.edu.tr (H.M.F.)
[2] Department of Medical Services and Techniques, İstanbul Gedik University, Istanbul 34876, Türkiye; parug.duru@gedik.edu.tr
* Correspondence: eng.noor85.noor85.n8n8@gmail.com or 213720601@ogr.altinbas.edu.tr

Abstract

Due to increasing human activities underwater, there is a growing demand for high-speed underwater optical communication (UOWC) data links for security surveillance, environmental monitoring, pipeline inspection, and other applications. Line-of-sight communication is impossible under certain conditions due to misalignment, physical obstructions, irregular usage, and difficulty adjusting the receiver orientation, especially when used in environments with mobile users or submerged sensor networks. Therefore, non-line-of-sight (NLOS) optical communication is used in this study. Advanced modulation schemes—quadrature amplitude modulation and orthogonal frequency-division multiplexing (QAM-OFDM)—were used to transmit the signal underwater between two network nodes. QAM increases the data transfer rate, while OFDM reduces dispersion and inter-symbol interference (ISI). The proposed UOWC system is investigated using a 532 nm green laser diode (LD). Reliable high-speed data transmission of up to 15 Gbps is achieved over horizontal distances of 134 m, 43 m, 21 m, and 5 m in four different aquatic environments—pure water (PW), clear ocean (CLO), coastal ocean (COO), and harbor II (HarII), respectively. The system achieves effectively error-free performance within the simulation duration (BER < 10^{-9}), with a received optical signal power of approximately −41.5 dBm. Clear constellation patterns and low BER values are observed, confirming the robustness of the proposed architecture. Despite the limitations imposed by non-line-of-sight (NLOS) communication and the diversity aquatic environments, our proposed architecture excels at underwater long-distance data transmission at high speeds.

Keywords: QAM-OFDM; underwater wireless communication; quadrature amplitude modulation; bit error rate (BER); UOWC; data transmission

Received: 24 December 2025
Revised: 6 January 2026
Accepted: 16 January 2026
Published: 22 January 2026

1. Introduction

1.1. Background and Motivation of Underwater Communication

Human activities are increasing the need for high-speed, high-data-rate underwater communication [1]. Conventional underwater acoustic communication is inherently limited in terms of bandwidth and data rate, making it unsuitable for high-speed applications [2]. RF underwater communication has a shorter propagation distance and a lower data rate [3]. UOWC technology is promising for underwater exploration due to its longer modulation bandwidth, energy efficiency, and propagation distance [4]. Scientific, oceanography, and military research focus on this technology [5].

1.2. Optical Propagation Characteristics in Underwater Environments

Water molecules' attenuation affects underwater light propagation. Underwater scattering and absorption cause most attenuation [6]. Clear or clean ocean water has the lowest blue-region attenuation [7]. Coastal water has the least attenuation [8]. Minerals, debris, and plankton are present in coastal water [9].

1.3. Review of High-Speed UOWC Experimental and Simulation Studies

Using a 450 nm LD, a 1.5 Gbps communication link was built over 20 m, with a low real-time data rate [10]. On–off keying modulation was used to send 2.70 Gbps data across 34.5 m for long-range underwater communication. Increased transmission distance induces reflection and multipath loss, lowering the BER [11].

32-QAM–OFDM was used to construct a 9.51 Gbps RGB-LD-based WDM data link across 10 m [12]. OFDM is commonly utilized to increase transmission capacity and spectral efficiency [13]. QAM and OFDM modulations are crucial because of their high spectral efficiency and low inter-carrier interference (ICI) [14].

Blue–green-zone transmission loss is lower; hence, Nakamura et al. used a 405 nm LD with OFDM to construct a 1.45 Gbps link spanning 5.4 m for smaller applications [15]. Xu et al. (2016) used compact blue LEDs to create an OFDM-based UOWC system that achieved 225.90 Mb/s and 231.95 Mb/s data rates over 2 m air and underwater channels, respectively, using 32 and 64-QAM OFDM, despite the shorter transmission distance and data rates [16].

A 5.5 Gbps air–water link over 26 m was constructed in 2017, employing 32 QAM–OFDM with 520 nm LD [17]. Improvements to m-QAM–OFDM UOWC systems were proposed for a 12.5 m tap-water channel. Clear water performs better; muddy water reduces transmission capacity [18]. QAM–OFDM modulation created a 6.23 Gb/s link with restricted DAC resolution, although transmission capacity can be enhanced [19].

1.4. OFDM System Design Considerations in Underwater Channels

OFDM modulation requires a cyclic-prefix (CP) length greater than the channel impulse response to eliminate the dispersion effect and ISI from multipath fading [20]. However, bandwidth, data rate, and transmission energy drop, so choosing the right CP-length is crucial for system performance [21].

1.5. Advanced Techniques: MIMO and Environmental Adaptation

The goal of study [22] was to improve the range and reliability of underwater wireless optical link communication under high-data-rate situations. Additionally, they adjusted critical optical link parameters such as seawater chlorophyll concentration to improve the prior approach of categorizing seawater environments into four types—pure, clear, coastal, and turbid—for light attenuation.

This helps adapt to regional seawater conditions. MIMO setups overcome underwater channel attenuation and turbulence to improve system performance. For modulation, this paper uses direct-detection optical OFDM and Quadrature Amplitude Modulation (QAM) due to OFDM's superior performance in underwater wireless optical communication.

The study designs its system model utilizing DDO-OFDM, QAM, and OptiSystem 21.0 (Optiwave Systems Inc., Ottawa, ON, Canada). MATLAB R2022b (MathWorks, Natick, MA, USA; https://www.mathworks.com) simulates chlorophyll's impact on aquatic life and evaluates the Bit Error Rate (BER) and communication distance under different MIMO settings. With a BER of 10^{-4}, the suggested system may reach a maximum distance of 55 m for a 1×1 SISO and 140 m for a 4×4 MIMO. At a BER of 10^{-6}, the 1×1 SISO can reach a maximum distance of 48 m, while the 4×4 MIMO can reach 135 m. MIMO's increased

effective communication range shows its performance improvement and strong application prospects [22].

1.6. Recent Applications and Emerging Trends in UOWC

In [23] noted that communication technology will help researchers analyze climate change by monitoring biological, biogeochemical, evolutionary, and ecological changes in marine and oceanic ecosystems. Submarines, ships, buoys, divers, underwater sensor networks, and crewless underwater vehicles must operate efficiently. Underwater acoustic communication technology cannot provide high data rates for comprehensive inquiry and monitoring for these conditions and facilities. Laser wireless communication is a viable solution to this problem. This research designs and tests an underwater optical communication link that can communicate over 130 m horizontally at a depth of 40 m. At 15 Gbps and using differential quadrature-phase shift keying and orthogonal frequency division multiplexing–quadrature amplitude modulation, the proposed system is rigorously tested under clear ocean circumstances.

Study [24] reviewed underwater VLC fundamentals, environmental effects (scattering and absorption), and dynamic water parameters. We show that conventional methods outperform adaptive and hybrid modulation strategies (QAM-OFDM achieving 4.92 Gbps over 1.5 m). We cover security issues and practical applications, including underwater exploration, autonomous vehicle control, and environmental monitoring. Experimental results demonstrate that UVLC can transcend traditional restrictions, with 500 Mbps over 150 m utilizing PAM4 modulation. Quantum communication with Reconfigurable Intelligent Surfaces (RISs) could improve performance by 40% in turbulent environments.

1.7. Limitations of Existing UOWC Studies

Through rigorous experimentation, UOWC systems have made great strides but still largely focus on line-of-sight (LOS) setups, limited ranges, and simplified aquatic environments in most studies. Furthermore, the literature is mainly composed of experimental previews or theoretical considerations revolving around a single water type, making performance conclusions less applicable to realistic underwater conditions.

On the other hand, QAM-OFDM and other advanced modulation schemes have been investigated thoroughly for terrestrial and free-space optical links but have not been systematically studied for long-range, high-speed NLOS underwater optical communication [25]. The interaction between scattering-dominated NLOS propagation, diverse water types, and high-data-rate transmission remains insufficiently addressed in terms of system performance metrics such as the BER and achievable transmission distance.

Hence, a research gap is evident in the comprehensive modeling and performance evaluation of high-speed NLOS UOWC systems across multiple aquatic environments using a unified simulation platform.

1.8. Aim and Overview of the Proposed NLOS UOWC System

This work aims to develop a 532 nm-operating green laser diode (LD) system for wireless UOWC, allowing for data transfer speeds up to 15 Gbps. The utilized technique is quadrature amplitude modulation (QAM) with orthogonal frequency division multiplexing (OFDM). It is well known for its strength in dispersive channels and its ability to generate high spectral efficiency. The combination OFDM and QAM produces great performance under conditions of complicated aquatic channels, including dispersion and scattering. The solution improves BER performance. Despite the constraints of NLOS and varied aquatic environments, our proposed architecture excels at long-distance data transfer at high data speeds in underwater environments.

A non-line-of-sight (NLOS) UOWC system with the ability to deliver ultra-high data rates over extended horizontal distances is introduced in this study, in contrast to most underwater optical wireless communication (UOWC) studies that focus on line-of-sight (LOS) configurations, short transmission distances, or limited aquatic environments.

Unlike past studies that analyzed a single water type or relied on experimental demonstrations over short ranges, this work systematically assesses the performance of a high-speed (15 Gbps) NLOS UOWC link across four different aquatic environments—pure water, clear ocean, coastal ocean, and harbor water—using a common OptiSystem-based simulation framework. The findings confirm reliable and effectively error-free transmission within the simulation duration (BER < 10^{-9}) over unprecedented NLOS horizontal distances of up to 134 m in pure water, affirming the strength and scalability of the proposed architecture. This thorough investigation provides a new perspective on the practical implementation of long-range, high-speed NLOS underwater optical communication systems under diverse real-world water conditions.

2. System Model and Simulation Setup

Attenuation is a well-established phenomenon that occurs due to absorption and scattering in water for underwater optical communications, according to previous studies. Seawater contains some contaminants, but their effect on attenuation in the visible spectrum, particularly in the blue and green regions, is much less. Both the scattering coefficient (b(λ)) and the absorption coefficient (a(λ)) affect how light is decomposed in seawater. Therefore, a high level of impurities degrades transmission quality. To facilitate high-speed communications, the wavelength must be carefully chosen. Equation (1) mathematically expresses the relationship between light propagation and attenuation (c(λ)) to describe the attenuation phenomenon quantitatively. This formula is fundamental to understanding and improving underwater optical communication systems, improving their performance in challenging aquatic environments [23,26]:

$$c(\lambda) = \alpha(\lambda) + \beta(\lambda) \quad (1)$$

where $\alpha(\lambda)$ is the absorption coefficient, $\beta(\lambda)$ is the scattering coefficient, and λ is the wavelength.

Absorption is the dominant factor in pure seawater, where a low scattering coefficient prevents the beam from diverging. Clear ocean water contains fewer suspended particles, which affects scattering. High levels of plankton, debris, and mineral concentrations in coastal waters contribute to absorption and scattering.

Table 1 shows typical values for the various coefficients ($\alpha(\lambda)$ and $\beta(\lambda)$) when using a 532 nm laser.

Table 1. Attenuation type [27].

Types of Water	Attenuation Type at 532 nm		
	Absorption Coefficient $\alpha(\lambda)$ (m^{-1})	**Scattering Coefficient $\beta(\lambda)$ (m^{-1})**	**$c(\lambda)$ (m^{-1})**
PW	0.0405	0.0025	0.043
CLO	0.114	0.037	0.151
COO	0.179	0.219	0.398
HarII	0.366	1.824	2.19

Our underwater wireless optical channel operates in NLOS mode, meaning a direct line of sight is unnecessary. Figure 1 illustrates the depth of the transmitter (represented by

h) and the depth of the receiver (represented by *x*). The symbol representing the angle of incidence is θ_1. The critical angle is θ_C.

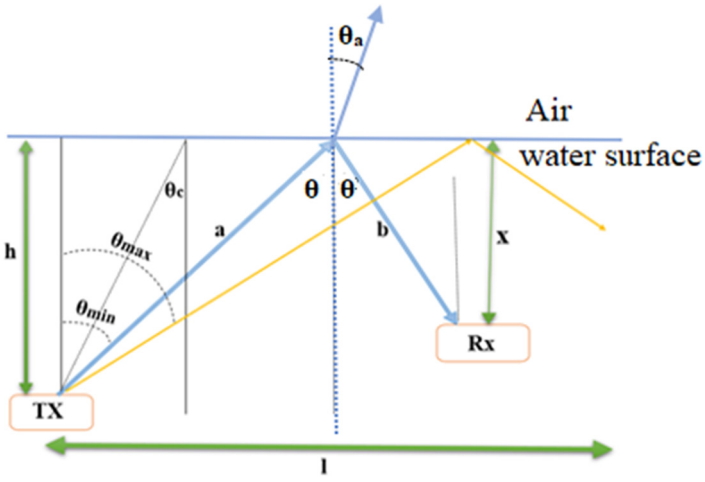

Figure 1. Archetypal NLOS configuration.

As shown in Figure 1, the transmitter emits a laser beam as a light cone directed upwards, with two outer angles (θ_{min} and θ_{max}). Total internal reflection (TIR) can occur when light travels from a medium with a higher refractive index to a medium with a lower refractive index. For example, when a light signal travels through water to the surface, it is completely reflected if its angle of incidence is greater than the critical angle. To calculate the critical angle, the formula of Snell's law is used [28]:

$$\mathrm{n}\,\sin(\theta) = \mathrm{n}_a\,\sin(\theta_a) \tag{2}$$

where n is the refractive index of water (≈ 1.33), θ is the angle of incidence of the ray at the water surface, n_a is the refractive index of air (≈ 1), and θ_a is the transmitted angle, as seen in Equation (3):

$$\Theta_c = \sin^{-1}(\mathrm{n}_a/\mathrm{n}) = \sin^{-1}(1.0003/1.333) \approx 48.6^\circ \tag{3}$$

In Figure 1, "a" symbol represents the time the transmitted beam takes to reach the water's surface. Like the original beam, the reflected beam's distance to the receiver is denoted as "b". To indicate the separation of the two planes, we use the letter "l". Equations (4) and (5) express a way to describe the received optical power when no line of sight is present, as seen in [25,26]

$$\begin{aligned} \mathrm{P}_{Rx} = \mathrm{P}_{Tx}\eta_{Tx}\eta_{Rx}\left(\frac{\mathrm{A}_{rec}\cos(\theta)}{\mathrm{A}_{ann}}\right) \times \mathrm{e}^{-(\mathrm{x}+\frac{\mathrm{h}}{\cos\theta})\mathrm{c}(\lambda)} \times 0.5 \\ \left[\left(\frac{\tan(\theta_a-\theta)}{\tan(\theta_a-\theta_C)}\right)^2 + \left(\frac{\sin(\theta-\theta_a)}{\sin(\theta+\theta_a)}\right)^2\right],\ \theta_{min} \le \theta < \theta_c \end{aligned} \tag{4}$$

$$\mathrm{P}_{Rx} = \mathrm{P}_{Tx}\eta_{Tx}\eta_{Rx}\left(\frac{\mathrm{A}_{rec}\cos(\theta)}{\mathrm{A}_{ann}}\right) \times \mathrm{e}^{-(\mathrm{x}+\frac{\mathrm{h}}{\cos\theta})\mathrm{c}(\lambda)}, \theta_{\min} \le \theta < \theta_C \tag{5}$$

In this context, P_{Tx} corresponds to the average optical power of the transmitter, η_{Tx} to the optical efficiency of the transmitter, η_{Rx} to the optical efficiency of the receiver, θ to the incident angle between the incident $\mathrm{T_X}$ ray and the plane perpendicular to the water's surface, and θ_a is the transmission angle between the refracted $\mathrm{T_X}$ ray and the plane perpendicular to the water's surface. It is calculated by taking the receiver aperture area

(A_{rec}) and multiplying it by the illuminated annular area (A_{ann}) at the sea surface. It can be expressed as Equation (6) [26]:

$$A_{ann} = 2\pi(x + h)^2[\cos(\theta_{min}) - \cos(\theta_{max})] \quad (6)$$

When calculating the value of P_{Rx}, the value of the BER can be calculated using Equation (7):

$$BER \approx \exp\left(-\frac{2P_{Rx}E}{B}\right) \quad (7)$$

where P_{Rx} is the received optical power, B is the bit rate, and E is the energy of the LD.

It must be emphasized that Equation (7) is an approximate analytical expression that is meant to be used only for illustrating the general relationship between the received optical power, bit rate, and noise in the system. The exact bit error rate (BER) values reported in this work are obtained from directly within the OptiSystem simulation environment, which internally simulates optical OFDM detection, noise sources, and receiver impairments. Thus, Equation (7) is applied for conceptual insight rather than as a rigorous theoretical derivation of the simulated BER performance.

Underwater optical wireless communication (UWOC) systems benefit more from non-line-of-sight (NLOS) configurations than line-of-sight (LOS) ones due to their ability to keep communication going even when obstacles are present. These topologies are more suited to changing underwater conditions because of the increased node placement and alignment leeway. They are the go-to choice when direct communication is not an option. Reflection and refraction techniques are crucial for indirect signal routing in these communication environments. Because of this, communication can continue uninterrupted if a direct connection between the sender and the recipient is unavailable. This attribute is crucial because of the importance of dependability, safety, and flexibility in underwater applications. Straight routes are restricted by barriers such as underwater terrain (e.g., coral reefs, rocks, and underwater caverns) and robots or vehicles that operate underground, in addition to particles in suspension or marine life. Lastly, differences in temperature and water density were previously found [29,30].

Figure 2 illustrates a model of the proposed underwater optical wireless communication (UOWC) system, based on OptiSystem simulations, that takes into account variations in horizontal distances between the transmitter and receiver, as well as variations in aquatic environments in NLOS communication. These variations significantly affect the received signal strength and bit error rate (BER) of UOWC systems. The system consists of three main parts: the transmitter, the aquatic channel, and the receiver.

2.1. Transmitter

The proposed transmitter features a 15 Gbps pseudo-random binary sequence (PRBS) data generator, followed by 4-QAM modulation, where each symbol carries two bits of information. As a compromise between noise resistance and modulation efficiency, a square constellation is used to disperse the symbols in the signal space. The signal is fed into an OFDM module to separate the data into smaller packets. The inverse fast Fourier transform (IFFT) method transforms the signals from the frequency domain to the time domain. This process significantly mitigates inter-symbol interference (ISI), since each sub-frequency is straight across from the others. This fortifies the system against channel interference and temporal dispersion [31]. A 532 nm green CW-LD laser was utilized [26]. Optically modulating the data with a Mach–Zehnder modulator (MZM) is the next step for the CW laser. End-user data is received by means of the water channel.

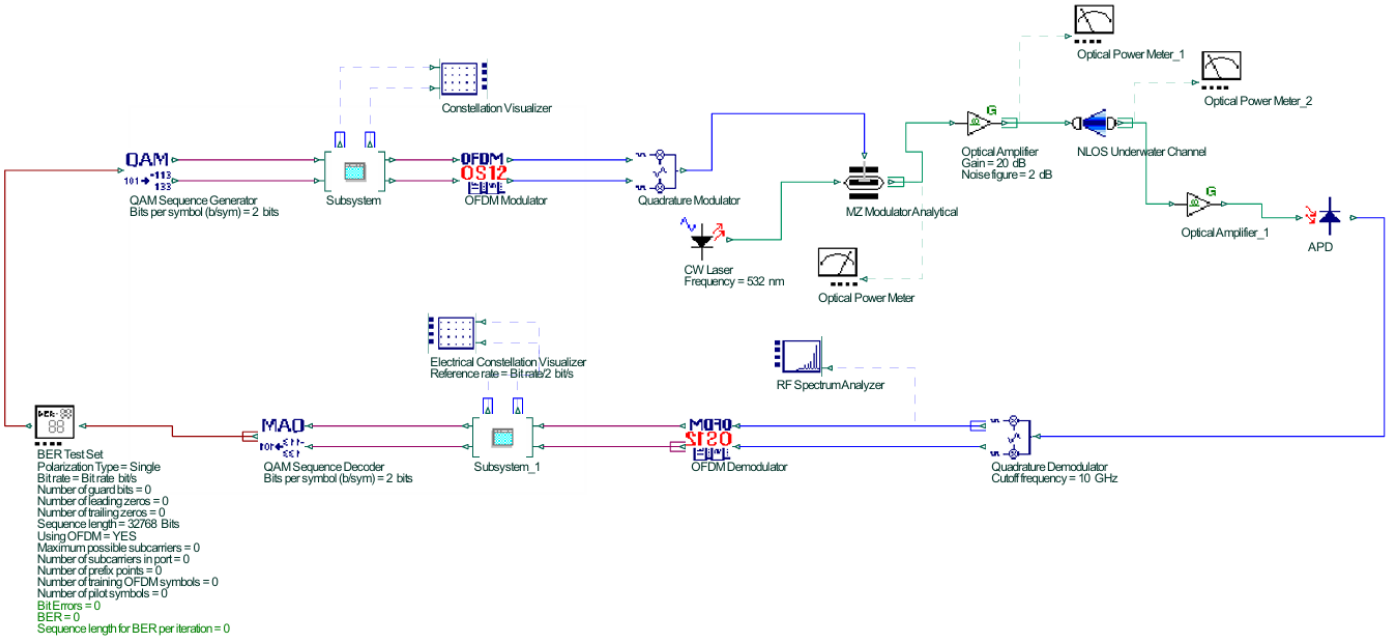

Figure 2. Block diagram of the proposed simulation system.

Solid lines represent the main signal flow, dashed lines indicate monitoring and visualization paths, and arrows show the direction of signal propagation. Different colors are used to distinguish between electrical and optical signal paths and to separate transmitter, channel, and receiver sections.

2.2. Water Channel

Over various aquatic habitats (PW, CLO, COO, and HarII), the signal was sent in non-line-of-sight (NLOS) manner. We adjusted the horizontal distance between the two devices depending on the setting. There was a salinity of 3.5%, a temperature of 10 °C, a transmit aperture of 5 cm, and a reception aperture of 20 cm. Optical communication devices find NLOS to be one of the most difficult conditions to operate in. Underwater optical communications suffer from poor received power and bit rate due to attenuation caused by scattering and dispersion. Therefore, to make sure the signal reached the receiver, an optical amplifier was positioned both before and after the water channel.

2.3. Receiver

An avalanche photodiode (APD) at the receiver side picks up the optical signal sent out and turns it into an electrical signal. The first step in processing incoming signals is transforming the photon stream into an electron stream [32]. An OFDM demodulator applies fast Fourier transform (FFT) to the received electrical signal, transforming it from the time domain to the frequency domain. A QAM sequence decoder is used to decipher the QAM signal. Based on the number of bits per symbol in this circuit, which is 2 bits, it turns the signal into digital data. After that, the signal is forwarded to the BER rate set, which determines the BER rate. Table 2 provides more details by listing the input parameters utilized by the suggested system. For precise modelling and analysis of the proposed QAM-OFDM-based UOWC system, OptiSystem simulation software is used for system evaluation. This study's comprehensive performance evaluation considers various underwater conditions and their effects on signal transmission quality [31,33].

Table 2. The components of the simulation used in the suggested system.

Component's Name	Description	Input Parameter Values
Transmitter part	Pseudo-random bit generator	Bit rate = 15 Gbps
	QAM	Bits per symbol = 2 bits/symbol (4-QAM) Constellation type = square/rectangular
	OFDM modulator	No. of subcarriers = 512 Position array = 256 FFT points = 1024 DAC interpolation = cubic
	LD	CW laser wavelength = 532 nm Power = 23 dBm Line width = 0.15 MHz Phase = 0°
	MZM	Extinction ratio = 30 dB
Transmission medium	Optical amplifier	Gain = 20
	Water channel	Type of underwater communication = NLOS n = 1.33, n_a = 1 θc = 48.6° Temperature = 10 °C Salinity = 3.5% Attenuation, according to the type of aquatic environment, as shown in Table 1 Transmitter aperture = 5 cm Receiver aperture = 20 cm
Receiving part	APD	Dark current = 10 nA Responsivity = 1 A/W Thermal noise = 10^{-22} W/Hz Shot noise distribution = Gaussian
	OFDM demodulator	No. of subcarriers = 512 Position array = 256 FFT points = 1024 DAC interpolation = cubic
	QAM sequence decoder	Bits per symbol = 2 bits/symbol (4-QAM) Constellation type = square/rectangular
Measurement's component	Optical power meter BER rate set	

3. Results

A 15 Gbps underwater optical communication system is designed in this research paper. Bit error rates (BERs) and constellation schemes are used to study the effects of different aquatic factors. Figures 3–6 display the BER values for each aquatic environment (PW, CLO, COO, and HarII) according to the maximum transmission distance between the transmitter and receiver. The study delves into the system performance over different distances by analyzing the constellation schemes and BER values. The combination of BER values and constellation schemes can measure system performance. Effectively error-free transmission within the simulation duration is indicated by BER values below 10^{-9}. Tables 3–6 show the results of measuring the BER and received power using a power meter at different horizontal transmitter–receiver distances in each aquatic environment (PW, CLO, COO, and HarII).

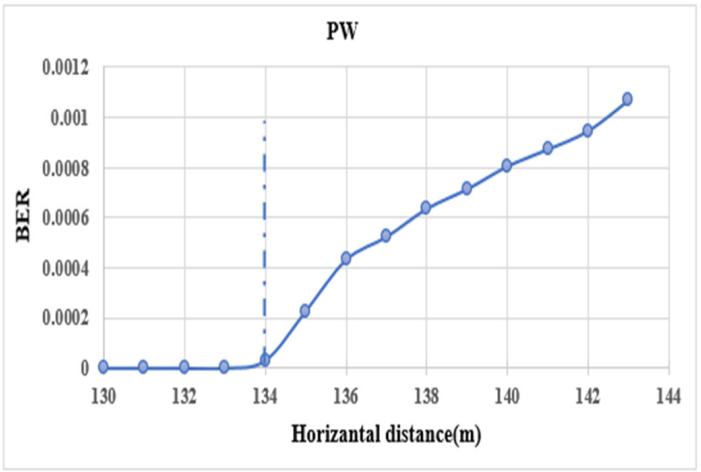

Figure 3. Bit error rate (BER) versus horizontal transmission distance at 15 Gbps using QAM-OFDM in pure water (PW).

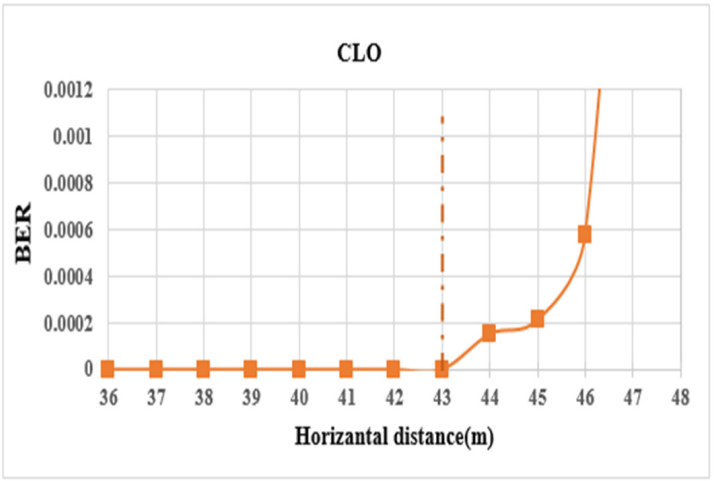

Figure 4. Variation of BER with underwater transmission distance at a 15 Gbps data rate using QAM-OFDM for CLO.

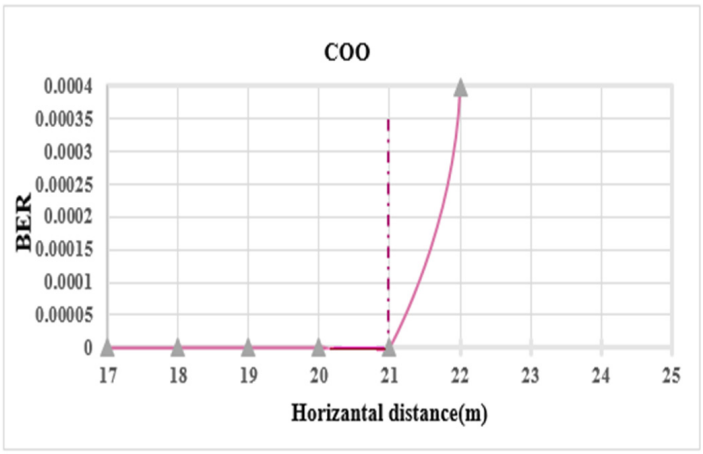

Figure 5. Variation of BER with underwater transmission distance at a 15 Gbps data rate using QAM-OFDM for COO.

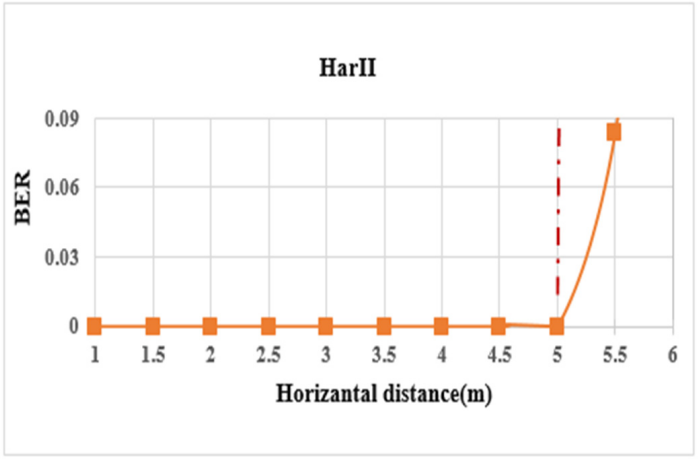

Figure 6. Variation of BER with underwater transmission distance at a 15 Gbps data rate using QAM-OFDM for HarII.

Table 3. Received power with BER when changing the distance between the transmitter and receiver in PW.

Horizontal Distance (m)	Power (dBm)	BER
130	−40.757	0
131	−40.8323	0
132	−41.3825	0
133	−41.3936	0
134	−41.4541	3×10^{-5}
135	−41.5629	0.000227246
136	−41.783	0.000431904
137	−41.9006	0.000523457
138	−42.4312	0.000635693
139	−42.6626	0.000713623
140	−42.8331	0.00080501
141	−42.8584	0.00087246
142	−43.4163	0.000946045

Table 4. Received power with BER when changing the distance between the transmitter and receiver in CLO.

Horizontal Distance (m)	Power (dBm)	BER
35	−35.2309	0
36	−36.5151	0
37	−37.3386	0
38	−37.7074	0
39	−38.122	0
40	−38.9394	0
41	−39.4682	0
42	−40.1238	0
43	−41.53	0
44	−42.0192	0.000152588
45	−42.8382	0.000213623
46	−43.4017	0.000579834
47	−44.0884	0.00363159
48	−44.6999	0.0102234

Table 5. Received power with BER when changing the distance between the transmitter and receiver in COO.

Horizontal Distance (m)	Power (dBm)	BER
17	−32.4576	0
18	−34.6212	0
19	−37.1023	0
20	−38.4662	0
21	−40.2477	0
22	−42.2548	0.000396729
23	−44.3844	0.00585938
24	−46.4428	0.0372009
25	−48.1581	0.130859
26	−49.5106	0.238922
27	−52.0814	0.296051
28	−53.6711	0.366791
29	−55.2768	0.413879
30	−57.6859	0.441681

Table 6. Received power with BER when changing the distance between the transmitter and receiver in HarII.

Horizontal Distance (m)	Power (dBm)	BER
1	−15.4642	0
1.5	−16.586	0
2	−16.9806	0
2.5	−17.2305	0
3	−21.9132	0
3.5	−26.9122	0
4	−32.0842	0
4.5	−37.2134	0
5	−42.0151	2.8×10^{-5}
5.5	−46.4622	0.083313
6	−52.1312	0.298431
6.5	−56.8201	0.432678
7	−61.5243	0.478485
7.5	−67.0302	0.493164

The bit error rate (BER) as a function of the horizontal transmission distance (in meters) in an OFDM-QAM UOWC underwater optical communication system is illustrated in Figure 3. We can see the horizontal distance between the two nodes on the *x*-axis in this graph. The bit error rate (BER) on the *y*-axis shows the communication quality. The graph can be examined for the first region, which extends from 1 m to 134 m.

According to Figures 4–6, the first region (before the dotted line) depicts a range of 1–43 m for clear ocean, 1–22 m for coastal ocean, and 1–5 m for harbor II conditions, respectively. Figures 3–6 show simulation results for four situations, all with BER values close to zero within the considered simulation duration. For the four water conditions, the maximum achievable distance of the system was 134, 43, 21, and 5 m for PW, CLO, COO, and HarII, respectively. The BER is significantly affected by water type, the horizontal distance between the two devices, and other factors. Due to increased scattering and absorption, BER values are higher [30,34,35].

In addition to the BER analysis, Figure 7 presents the constellation diagram of the OFDM-QAM system response under pure underwater conditions at a horizontal range of 134 m, confirming the reliable system performance observed in Figures 3–6.

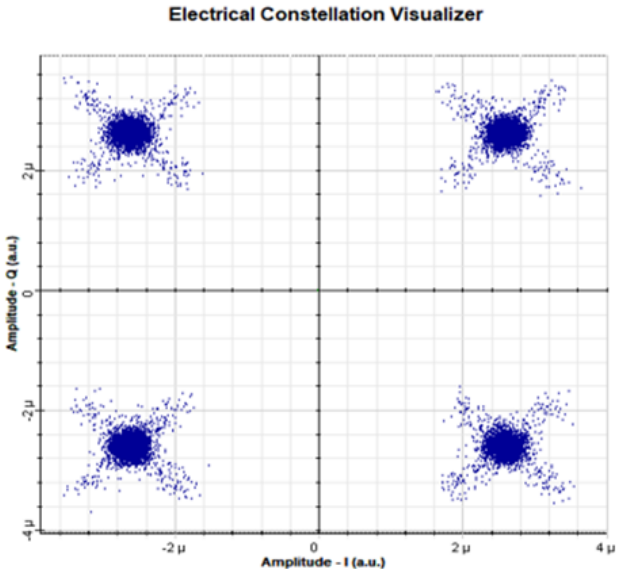

Figure 7. The constellation diagram of the OFDM-QAM system response in pure underwater conditions for a horizontal range of 134 m.

As seen in Figure 8, a slight rise in the receive BER causes the array points to disperse about their optimal locations, suggesting a somewhat robust system. Although there is some noise in the channel, the distribution of points is still distinct and unambiguous; therefore, the bit error rate (BER) is acceptable [36].

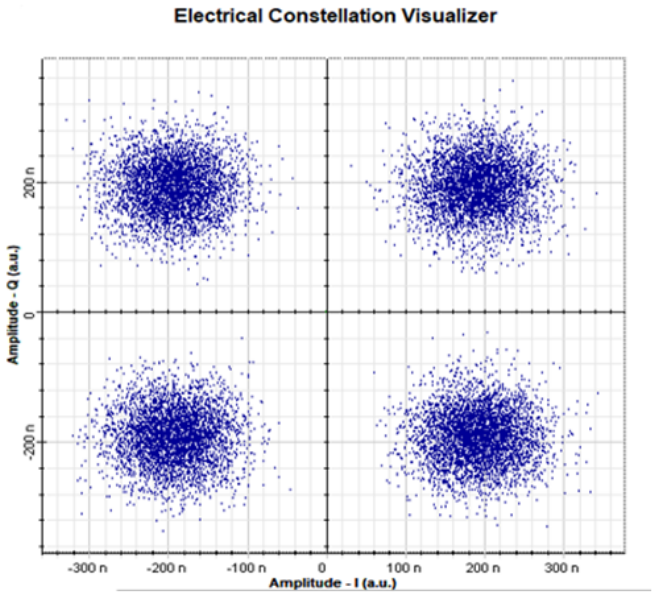

Figure 8. The constellation diagram of the OFDM-QAM system response in pure underwater conditions for a horizontal range of 137 m.

Figure 9 shows that the four groups of dots for QAM symbols start to blend and converge as the BER and horizontal distance between the sender and receiver grow. Because the constellation becomes less distinct, the system starts to have trouble telling

symbols apart. As a result, signal degradation, water dispersion, and noise all increase with distance [36,37].

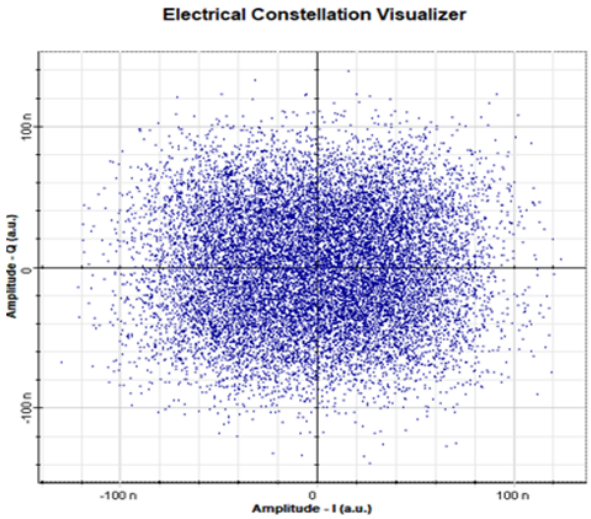

Figure 9. The constellation diagram of the OFDM-QAM system response in pure underwater conditions for a horizontal range of 145 m.

Figures 10–13 and Tables 3–6 illustrate the results of measuring received power using an optical power meter at different horizontal distances between the transmitter and receiver in each aquatic environment—namely, pure water, clear ocean, coastal ocean, and harbor II. Based on the observed relationship between the two variables, system performance declines sharply as the bit error rate (BER) rises and the received power falls below about −43 dB. The findings prove that horizontal distance, BER, and received power are the most important factors determining an underwater optical communication system's performance in a coastal setting. These findings are highly instructive for the design of UWOC systems, particularly in difficult situations such as coastal areas with considerable attenuation. Regardless of the aquatic environment (PW, ClO, COO, or HarII), the system maintains signal quality over extended distances and shows good BER performance.

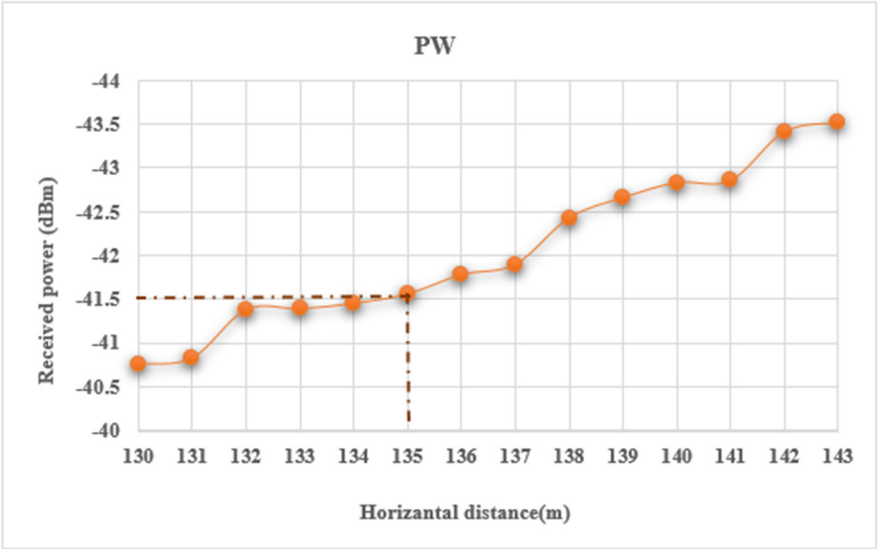

Figure 10. Received optical power versus horizontal transmission distance in pure water (PW). The solid orange line represents the simulated received optical power variation, while the dotted line indicates the maximum achievable transmission distance.

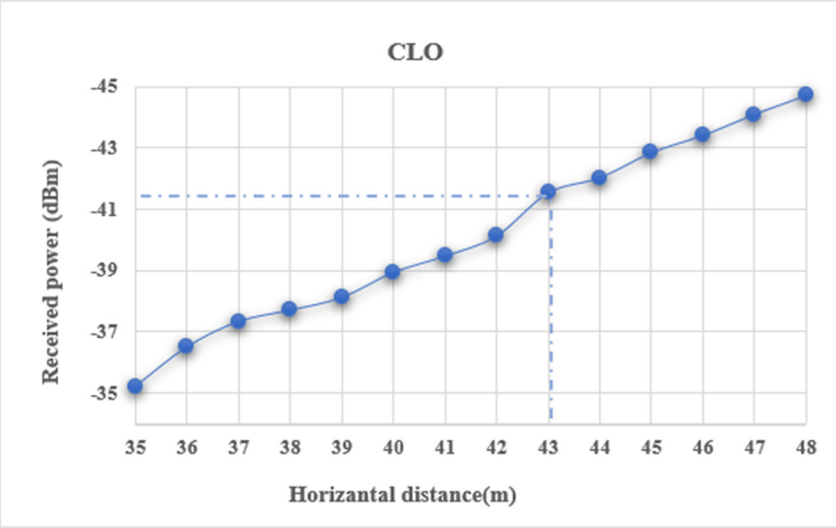

Figure 11. Received power versus horizontal distance for CLO. The solid blue line represents the simulated received optical power variation, while the vertical dotted line indicates the maximum achievable transmission distance.

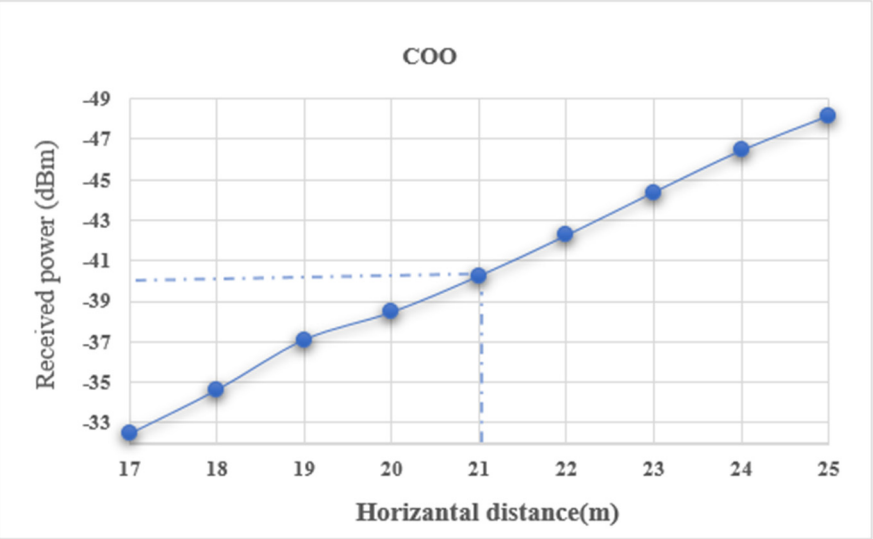

Figure 12. Received power vs. horizontal distance for COO.

Figure 10 reflects the signal quality of the underwater optical system, illustrating the relationship between the horizontal transmission distance and the received optical signal power in the PW aquatic environment. The received power in the first region (between 130 and 134 m) ranges between −40 dBm and −41.5 dBm, indicating relatively strong signals that can maintain high transmission quality. As shown in Figure 10, the received power helps achieve a very low bit error rate (BER), indicating that the laser beam is well and evenly distributed over this distance. Due to noise in the system, the received signal power decreases in the second region (after 134 m). In practice, the received signal becomes noise-dominated rather than presenting as a real signal. The significant absorption and scattering in the underwater environment, especially in NLOS systems, is the main reason for this breakdown. The light energy concentration decreases with increasing horizontal distance due to the dispersion of the green beam (532 nm) [37].

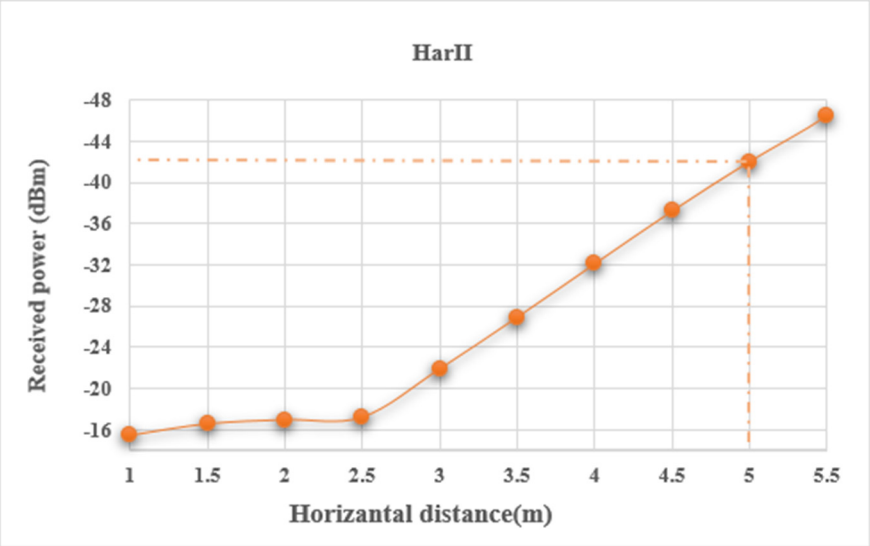

Figure 13. Received power vs. horizontal distance for HarII.

Figure 11 illustrates the relationship between the horizontal transmission distance and the received optical signal strength in a CLO aquatic environment. The power received in the first zone (between 35 and 43 m) ranges between −40 dBm and −41.5 dBm, and the received power level is sufficient to sustain reliable high-quality transmission. As seen in the previous graph, this degree of power helps achieve a very low bit error rate (BER), indicating that the laser beam is well distributed over this distance. Due to noise in the system, the power decreases in the second zone (after 43 m). In practical terms, this means that the receiver now transmits a noisy signal rather than just a real signal. The decrease in the BER shown in the previous graph and this decrease in amplitude are the same. The significant absorption and scattering in the underwater environment, especially in non-line-of-sight (NLOS) systems, are the main reasons for this breakdown [38].

Figure 12 illustrates the relationship between the horizontal transmission distance and the received optical signal strength in the COO aquatic environment. The received power in the first zone (between 17 and 21 m) ranges between (−33) and (−41) dBm, indicating relatively strong signals that can maintain high transmission quality. As seen in the previous graph, this degree of power helps achieve a very low bit error rate (BER), indicating that the laser beam is well distributed over this distance. Due to noise in the system, the power decreases in the second zone (after 21 m). In practical terms, the received signal becomes noise-dominated rather than information-bearing. The significant absorption and scattering in the underwater environment, especially in non-line-of-sight (NLOS) systems, are the main reasons for this breakdown. The optical energy concentration decreases with increasing horizontal distance because the green (532 nm) beam is scattered.

Figure 13 shows how the power of an optical signal received in the HarII aquatic environment is related to the horizontal transmission distance. Generally, strong signals capable of maintaining good transmission quality are indicated by the first region's received power (around 1 to 5 m) and vary from −16 dBm to −24 dBm. This power level allows for a low bit error rate (BER). Due to system noise, the power drops continuously in the second area (beyond 5 m). In practice, this implies that the receiver is no longer transmitting a pure signal but, rather, one accompanied by noise. Most notably, in non-line-of-sight (NLOS) systems, this failure is caused by the high levels of absorption and scattering in the underwater environment. Due to scattering, the optical energy concentration drops as the horizontal distance increases for the green (532 nm) beam [37,39].

4. Discussion

In the last few years, research on underwater optical wireless communication (UOWC) has mainly focused on line-of-sight (LOS) transmission cases with short distances and on the use of different modulation techniques to facilitate spectral efficiency and system reliability. QAM-OFDM is one of the modulation techniques that has obtained the highest acceptance, mainly because of its resistance to dispersion and inter-symbol interference. For example, a high-speed QAM-OFDM-based UOWC system with a blue/green laser diode was demonstrated under controlled LOS conditions by Oubei et al. [28]. They managed to reach gigabit-class data rates over a restricted region of transmission [28]. This study demonstrates the ability of QAM-OFDM to support high-capacity underwater optical links but does not consider its application to non-line-of-sight (NLOS) and scattering-dominated underwater environments.

In parallel, new PAM-based UOWC systems have come up lately; these systems have the potential to make the whole system less complicated and to enhance the sensitivity of the receiver. A recent study published in Photonics is given as a typical example where PAM modulation was used to achieve reliable underwater optical transmission under LOS conditions and at moderate link distances [30]. Even if PAM-based techniques are easier to implement, their performance is usually more affected by noise, dispersion, and channel-induced distortions, especially when higher data rates are used.

In contrast to this, the current study incorporates QAM-OFDM transmission into NLOS underwater optical channels while also conducting a thorough analysis of the performance of the system in four different artificial aquatic environments that include pure water and highly turbid harbor water. The results obtained so far have shown that QAM-OFDM is very robust when it comes to scattering and attenuation effects, which made it possible to carry out error-free transmissions within the simulation duration (BER < 10^{-9}) at a data rate of 15 Gbps over a distance of 134 m in pure water during the simulation period. These transmission distances are much greater than those observed in most UOWC research, particularly with respect to NLOS scenarios. These results indicate that the proposed system not only competes with but also outperforms both conventional QAM-OFDM LOS systems and PAM-based UOWC approaches in terms of speed, range, and reliability in NLOS underwater optical communication.

4.1. Modeling Assumptions and Physical Considerations

The NLOS channel modeling method implemented in this research is a reflection-dominated propagation mechanism that happens at the water–air boundary. This transmission path of indirect nature is the main one under the geometry used in this study. A smooth and calm water surface is presupposed; thus, the specular reflection according to Snell's law and the critical angle condition is permitted. Therefore, the surface reflection efficiency is implicitly reflected by the incident and refracted angles in the formula for the received optical power, while the changes in the surface due to wind or water turbulence are not modeled here.

The main loss mechanisms caused by non-line-of-sight (NLOS) propagation can be effectively captured by using the bulk attenuation coefficient that combines absorption and scattering for the different water types. However, this technique does not require any explicit angular scattering modeling. Nevertheless, the photon-scatter angular distribution and multiple scattering paths are still not explicitly resolved, and this may result in some inaccuracies in very long horizontal distances or under very turbid water conditions.

In this study, polarization effects are not taken into account, and unpolarized optical transmission and polarization-insensitive direct detection at the receiver are assumed. This assumption is quite practical for long-distance underwater optical communication, since

absorption and scattering mainly degrade the signal, and the effects related to polarization become of less importance. These modeling assumptions, in total, offer a framework that is both realistic and computationally efficient for the system-level performance evaluation of high-speed non-line-of-sight underwater optical wireless communication (NLOS UOWC) links while also explicitly indicating the physical limits of the proposed model.

4.2. Optical Amplification and Noise Considerations

Optical amplifiers are used at the beginning and the end of the underwater channel to counteract the optical losses that are very high due to absorption, scattering, and beam divergence in non-line-of-sight propagation situations. The choice of a fixed amplifier gain of 20 dB is made in the present research as a realistic compromise between the necessary power compensation and noise uplift. This gain level is frequently used in simulation-based UOWC studies to achieve received power levels that can be detected over long horizontal distances without pushing the system into a state of being dominated by excessive noise.

The fact that optical amplification results in an increase in spontaneous emission (ASE) noise, which can lower the signal-to-noise ratio (SNR) and, hence, affect the bit error rate (BER) performance, especially at long transmission distances, is indisputable. Nevertheless, in the context of the simulation framework used here, the main reasons for limited performance are still the underwater absorption and scattering losses instead of the noise from the amplifier. To this end, the amplifier is mainly used to bring the signal power up to the optimum level for direct detection, and its noise contribution is indirectly reflected in the BER increase, which occurs at the maximum achievable transmission distances.

Deep and thorough analytical modeling of ASE noise interacts with underwater channel impairments and definitely falls outside the scope of this work. Still, the presented results provide a fairly accurate system-level performance evaluation under amplified NLOS conditions. Further research might involve ASE noise modeling, gain optimization, and noise figure analysis to refine the BER predictions and decide on the most effective placement of energy-efficient amplifiers in real UOWC systems.

4.3. Limitations and Future Research Directions

Although the proposed QAM-OFDM-based NLOS UOWC system showed encouraging results for different water types, the study was performed under ideal and controlled simulation conditions. The modeling of an underwater optical channel was achieved by applying conventional absorption and scattering coefficients, and dynamic environmental effects like water flow disturbances, temperature gradient changes, and marine biological activities were not directly taken into account.

The present study also takes a single-point communication link as a model to analyze the basic system characteristics and performance limits. A discussion of multi-user communication scenarios and related access techniques is not included in this work. Such restrictions do not affect the credibility of the achieved results; on the contrary, they specify unambiguous paths for further research, which include the investigation of dynamic channel effects and multi-user transmission techniques, as well as experimental validation in the direction of practical NLOS UOWC system deployment.

Moreover, laser power stability, detector noise characteristics, optical amplifier non-idealities, and system energy consumption are practical hardware-related factors that are not included in the current simulation framework. Engineering these aspects and performing energy efficiency analysis would be the necessary steps for future experimental validation and prototype development, respectively.

5. Conclusions

The purpose of this research is to develop a non-line-of-sight (NLOS) underwater optical wireless communication (UOWC) system using the advanced modulation techniques of orthogonal frequency division multiplexing (OFDM) and quadrature amplitude modulation (QAM). A green laser diode at 532 nanometers was used, which is the optimal wavelength for penetrating water. The system's performance was tested in many types of water, including pure water, clear water, coastal water, and harbor water, by sending digital data at high speeds (up to 15 Gbps) over lengths of water ranging from 134 to 5 m. The research assessed the received optical power and the bit error rate (BER) to assess the system's performance in different non-line-of-sight (NLOS) scenarios.

A light signal was transmitted over an underwater horizontal distance of 134 m between the transmitter and receiver in pure water with error-free performance within the simulation duration (BER below 10^{-9}) and a received signal strength of approximately -41.5 dBm. In clear ocean conditions, reliable transmission was achieved over distances of up to 43 m. The broadcast distance was 21 m, and the received power was about -40 dBm in coastal ocean water. The signal was effectively broadcast to distance of 5 m in harbor II water, with a received power of about -42 dBm. The clear constellation diagrams and low BER values prove the effectiveness of the suggested approach.

With OFDM technology, dispersion and inter-symbol interference (ISI) were lessened, leading to better performance in terms of the bit error rate. Even in NLOS scenarios and across different aquatic habitats, the results show that the suggested approach performs better when transmitting data over long distances and at high rates underwater. An underwater optical communication (UOWC) system that used 532 nm green laser technology and combined QAM and OFDM techniques to transmit data was initially proposed in this work.

Author Contributions: Conceptualization, N.A.H.; Methodology, N.A.H. and İ.P.D.; Software, N.A.H.; Formal analysis, N.A.H.; Data curation, N.A.H.; Writing—original draft preparation, N.A.H.; Writing—review and editing, M.Ç., H.M.F., and İ.P.D.; Validation, H.M.F. and İ.P.D.; Supervision, M.Ç. and H.M.F.; Project administration, M.Ç.; All authors have read and agreed to the published version of the manuscript.

Funding: This research received no external funding.

Data Availability Statement: All relevant data are included within the paper.

Conflicts of Interest: The authors declare that they have no affiliations with or involvement in any organization or entity with any financial interest in the subject matter or materials discussed in this manuscript.

References

1. Bai, J.; Yang, S. A Combined PAPR Reduction Method by PTS Approach Based on Improved Particle Swarm Optimization. *Optik* **2021**, *232*, 166581. [CrossRef]
2. Zhang, L.; Tang, X.; Sun, C.; Chen, Z.; Li, Z.; Wang, H.; Jiang, R.; Shi, W.; Zhang, A. Over 10 Attenuation Length Gigabits-per-Second Underwater Wireless Optical Communication Using a Silicon Photomultiplier-Based Receiver. *Opt. Express* **2020**, *28*, 24968–24980. [CrossRef]
3. Islam, M.S.; Younis, M.; Mahmud, M.; Carter, G.; Choa, F.S. A Peak-Detection-Based OOK Photoacoustic Modulation Scheme for Air-to-Underwater Communication. *Opt. Commun.* **2023**, *529*, 129078. [CrossRef]
4. Wang, T.; Tian, R.; Zhu, R.; Jiang, L.; Tong, C.; Lu, H.; Song, Y.; Zhang, P. Improved Underwater Wireless Optical Communication Using a Passively Mode-Locked VECSEL. *Opt. Commun.* **2023**, *547*, 129850. [CrossRef]
5. Chen, D.; Zhang, X.; Fan, K.; Wang, J.; Lu, H.; Wang, Q.; Wu, S.; Hao, R.; Li, Z.; Jin, J. Experimental Demonstration of a Hybrid OFDMA/NOMA Scheme for Multi-User Underwater Wireless Optical Communication Systems. *Opt. Commun.* **2023**, *548*, 129823. [CrossRef]

6. Johnson, L.J.; Jasman, F.; Green, R.J.; Leeson, M.S. Recent advances in underwater optical wireless communications. *Underw. Technol.* **2014**, *32*, 167–175. [CrossRef]
7. Song, Y.; Lu, W.; Sun, B.; Hong, Y.; Qu, F.; Han, J.; Zhang, W.; Xu, J. Experimental demonstration of MIMO-OFDM underwater wireless optical communication. *Opt. Commun.* **2017**, *403*, 205–210. [CrossRef]
8. Schirripa Spagnolo, G.; Cozzella, L.; Leccese, F. Underwater optical wireless communications: Overview. *Sensors* **2020**, *20*, 2261. [CrossRef]
9. Gkoura, L.K.; Roumelas, G.D.; Sandalidis, H.E.; Nistazakis, H.G.; Vavoulas, A.; Tsigopoulos, A.D.; Tombras, G.S. Underwater Optical Wireless Communication Systems: A Concise Review. In *Turbulence Modelling Approaches—Current State, Development Prospects, Applications*; IntechOpen: London, UK, 2017. [CrossRef]
10. Shen, C.; Guo, Y.; Oubei, H.M.; Ng, T.K.; Liu, G.; Park, K.H.; Ho, K.T.; Alouini, M.-S.; Ooi, B.S. 20-Meter Underwater Wireless Optical Communication Link with 1.5 Gbps Data Rate. *Opt. Express* **2016**, *24*, 25502–25509. [CrossRef]
11. Fei, C.; Wang, Y.; Du, J.; Chen, R.; Lv, N.; Zhang, G.; Tian, J.; Hong, X.; He, S. 100-m/3-Gbps Underwater Wireless Optical Transmission Using a Wideband Photomultiplier Tube. *Opt. Express* **2022**, *30*, 2326–2337. [CrossRef]
12. Kong, M.; Lv, W.; Ali, T.; Sarwar, R.; Yu, C.; Qiu, Y.; Qu, F.; Xu, Z.; Han, J.; Xu, J. 10-m 9.51-Gb/s RGB Laser Diodes-Based WDM Underwater Wireless Optical Communication. *Opt. Express* **2017**, *25*, 20829–20834. [CrossRef]
13. Azarnia, G.; Sharifi, A.A. Clipping-Based PAPR Reduction of Optical OFDM Signals Using Compressive Sensing: Bayesian Signal Reconstruction Approach. *Opt. Fiber Technol.* **2021**, *64*, 102527. [CrossRef]
14. Li, Y.; Qiu, H.; Chen, X.; Fu, J. A Novel PAPR Reduction Algorithm for DCO-OFDM/OQAM System in Underwater VLC. *Opt. Commun.* **2020**, *463*, 125449. [CrossRef]
15. Nakamura, K.; Mizukoshi, I.; Hanawa, M. Optical Wireless Transmission of 405 nm, 1.45 Gbit/s Optical IM/DD-OFDM Signals through a 4.8 m Underwater Channel. *Opt. Express* **2015**, *23*, 1558–1566. [CrossRef] [PubMed]
16. Xu, J.; Kong, M.; Lin, A.; Song, Y.; Yu, X.; Qu, F.; Han, J.; Deng, N. OFDM-Based Broadband Underwater Wireless Optical Communication System Using a Compact Blue LED. *Opt. Commun.* **2016**, *369*, 100–105. [CrossRef]
17. Chen, Y.; Kong, M.; Ali, T.; Wang, J.; Sarwar, R.; Han, J.; Guo, C.; Sun, B.; Deng, N.; Xu, J. 26 m/5.5 Gbps Air–Water Optical Wireless Communication Based on an OFDM-Modulated 520-nm Laser Diode. *Opt. Express* **2017**, *25*, 14760–14765. [CrossRef]
18. Zhang, L.; Wang, H.; Shao, X. Improved m-QAM–OFDM Transmission for Underwater Wireless Optical Communications. *Opt. Commun.* **2018**, *423*, 180–185. [CrossRef]
19. Guo, Y.; Wang, X.; Fu, M. QAM–OFDM Transmission in Underwater Wireless Optical Communication System with Limited Resolution DAC. *Opt. Quantum Electron.* **2020**, *52*, 419. [CrossRef]
20. Arakawa, M.; Ochiai, H. On Throughput Optimization for Coded OFDM with Variable Cyclic Prefix Length. In Proceedings of the 20th International Symposium on Wireless Personal Multimedia Communications (WPMC), Bali, Indonesia, 17–20 December 2017; IEEE: New York, NY, USA, 2017; pp. 46–51.
21. Kotzsch, V.; Rave, W.; Fettweis, G. ISI analysis in network MIMO OFDM systems with insufficient cyclic prefix length. In *Proceedings of the 7th International Symposium on Wireless Communication Systems*; IEEE: New York, NY, USA, 2010; pp. 189–193. [CrossRef]
22. Wang, P.; Yang, G.; Yang, M.; Wu, Y. Performance analysis of underwater wireless optical communication system with mixed OFDM and QAM. In Proceedings of the 15th International Conference on Information Optics and Photonics (CIOP 2024), Xi'an, China, 11–15 August 2024; p. 24. [CrossRef]
23. Sahu, P.K.; Ghosh, D. Study and analysis of modulation schemes for underwater optical wireless communication. *J. Opt. Photonics Res.* **2024**, *2*, 27–35. [CrossRef]
24. Jayaweera, V.L.; Peiris, C.; Darshani, D.; Edirisinghe, S.; Dharmaweera, N.; Wijewardhana, U. Visible light communication for underwater applications: Principles, challenges, and future prospects. *Photonics* **2025**, *12*, 593. [CrossRef]
25. Zayed, M.M.; Shokair, M.; Elagooz, S.; Elshenawy, H. Non-Line-of-Sight (NLOS) Link Budget Analysis for Underwater Wireless Optical Communications (UWOCs). *Opt. Quantum Electron.* **2024**, *56*, 7. [CrossRef]
26. Al-Din, M.B.; Alkareem, R.A.S.A.; Ali, M.A.A. Transmission of 10 Gb/s for Underwater Optical Wireless Communication System. *J. Opt.* **2024**. [CrossRef]
27. Li, S.; Zhang, Z.; Zhang, Q.; Yao, H.; Li, X.; Mi, J.; Wang, H. Breakthrough Underwater Physical Environment Limitations on Optical Information Representations: An Overview and Suggestions. *J. Mar. Sci. Eng.* **2024**, *12*, 1055. [CrossRef]
28. Oubei, H.; Duran, J.; Janjua, B.; Wang, H.; Tsai, C.; Chi, Y.; Ng, T.K.; Kuo, H.; He, J.; Alouini, M.-S.; et al. 4.8 Gbit/s 16-QAM-OFDM Transmission Based on Compact 450-nm Laser for Underwater Wireless Optical Communication. *Opt. Express* **2015**, *23*, 23302–23309. [CrossRef]
29. Ali, M.A.A.; Shaker, F.K. Performance of an Underwater Non-Line-of-Sight (NLOS) Wireless Optical Communications System Utilizing LED. *J. Opt.* **2024**, *53*, 1429–1437. [CrossRef]
30. Fang, C.; Li, S.; Wang, Y.; Wang, K. High-Speed Underwater Optical Wireless Communication with Advanced Signal Processing Methods Survey. *Photonics* **2023**, *10*, 811. [CrossRef]

31. Matarneh, A.M.; Rwaidi, A.M.; Alja'afreh, S.S. Evaluating 60 GHz Band Underwater Optical Wireless Communication Performance Based on Low-Density Parity Check Coding under Diverse Water Conditions and Noise Levels. *IEEE Access* **2025**, *13*, 97129–97151. [CrossRef]
32. Kaushal, H.; Kaddoum, G. Underwater Optical Wireless Communication. *IEEE Access* **2016**, *4*, 1518–1547. [CrossRef]
33. Das, A.; Atta, R.; Pal, B.; Sarkar, N.; Santra, S.; Patra, A.S. 14 Gbps QAM–OFDM Optical Wireless Communication System Employing Pulse Shaping Technique in Coastal Water Environment with Optimization of Cyclic Prefix Length. *J. Opt.* **2024**, 1–10. [CrossRef]
34. Ke, X. Key Technologies in Underwater Optical Wireless Communication. In *Handbook of Optical Wireless Communication*; Springer: Singapore, 2024. [CrossRef]
35. Hua, M.; Liu, S.; Zhou, L.; Bünzli, J.C.; Wu, M. Phosphor-Converted Light-Emitting Diodes in the Marine Environment: Current Status and Future Trends. *Chem. Sci.* **2025**, *16*, 2089–2098. [CrossRef]
36. Sarkar, D.; Barua, B. Performance Analysis of Underwater Optical Wireless Communication System under Clear Oceanic Environment. *J. Opt. Commun.* **2025**. [CrossRef]
37. Ata, Y.; Kiasaleh, K. Analysis of Optical Wireless Communication Links in Turbulent Underwater Channels with Wide Range of Water Parameters. *IEEE Trans. Veh. Technol.* **2023**, *72*, 6363–6374. [CrossRef]
38. Hameed, S.M.; Sabri, A.A.; Abdulsatar, S.M. Filtered OFDM for Underwater Wireless Optical Communication. *Opt. Quantum Electron.* **2023**, *55*, 77. [CrossRef]
39. Arnon, S.; Kedar, D. Non-Line-of-Sight Underwater Optical Wireless Communication Network. *J. Opt. Soc. Am. A* **2009**, *26*, 530–539. [CrossRef] [PubMed]